Nonlinear self-excited forces for a bluff body in post-critical galloping

EACWE2022

8th European-African Conference on Wind Engineering

20-23 September 2022 | Bucharest, Romania

Nonlinear self-excited forces for a bluff body in post-critical galloping

Chaoqun Wang[1*)], Xugang Hua[2)], Claudio Mannini[3)], Zhengqing Chen[4)]

1) PhD candidate, Key Laboratory for Wind and Bridge Engineering of Hunan Province, College of Civil Engineering, Hunan University, China; CRIACIV / Department of Civil and Environmental Engineering, University of Florence, Italy, cqwang@hnu.edu.cn
2) Professor, Key Laboratory for Wind and Bridge Engineering of Hunan Province, College of Civil Engineering, Hunan University, China, cexghua@hnu.edu.cn
3) Assistant Professor, CRIACIV / Department of Civil and Environmental Engineering, University of Florence, Italy, claudio.mannini@unifi.it
4) Professor, Key Laboratory for Wind and Bridge Engineering of Hunan Province, College of Civil Engineering, Hunan University, China, zqchen@hnu.edu.cn

ABSTRACT: Self-excited aerodynamic forces during transverse galloping oscillations have not only nonlinear characteristics but, despite the high reduced wind velocity, may also present significant unsteady features. In this study, the characteristics of the lateral self-excited force for a bluff body in post-critical galloping are analysed in depth by inspecting force hysteresis loops obtained through CFD simulations. It is found that nonlinear characteristics become prominent with increasing vibration amplitude, while unsteady features remain significant at any vibration amplitudes. The mathematical model based on amplitude-dependent flutter derivatives is introduced for the unsteady galloping phenomenon, and it can be used in calculations of critical wind speed as well as post-critical response. In addition, the aerodynamic damping contour is calculated based on the force model, and it can be used to easily forecast the amplitude-wind speed curve of the bluff body with nonlinear structural damping.

Keywords: Post-critical oscillations, galloping, unsteady, nonlinear, self-excited force.

1. INTRODUCTION

In the authors' recent study of post-critical galloping of a bluff body (Wang et al., 2021), it has been found that the lift force during post-critical vibration presents both prominent unsteady and nonlinear characteristics even at a very high reduced wind velocity. Focusing on this issue, some theoretical analysis and discussion on the nonlinear lift force based on effective wind attack angle and order decomposition are given in this paper. Moreover, the mathematical model based on amplitude-dependent flutter derivatives (Tang, 2015) is introduced for the nonlinear galloping phenomenon, and the potential application of this force model in calculations of critical wind speed as well as post-critical response is discussed.

2. AERODYNAMIC FORCE OF POST-CRITICAL GALLOPING

2.1. Post-critical galloping of the bluff body

The main cables of a suspension bridge show various cross-sectional shapes with the evolution of construction phases, and they may suffer from severe galloping at certain conditions. The post-critical galloping behaviour of a main cable with a selected cross section (Figure 1) observed in a wind tunnel test was well reproduced through a CFD simulation (Wang et al., 2021). The single-

*) *Corresponding author*

degree-of-freedom dynamic model used in the CFD simulation is also depicted in Figure 1. A limit-cycle oscillation with a large vibration amplitude A = 3.99H, is reached after a build-up phase at reduced wind velocity U/fH = 299.6 and initial wind attack angle α = +2° (where U denotes the velocity of incoming flow, H denotes the height of the bluff body, f is the vibration frequency).

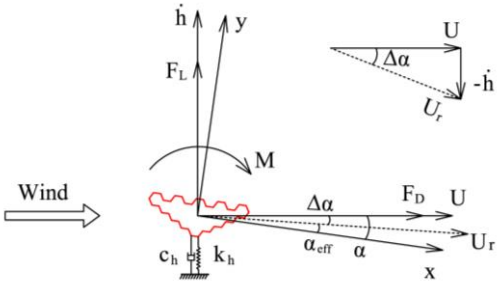

Figure 1. Selected cross section and dynamic model of a main suspension cable during construction.

2.2. Nonlinear aerodynamic force

In order to study the unsteady and nonlinear characteristics of the lift force, the hysteresis loops of the lift force at three different amplitudes (i.e., 0.42H, 2.40H and 3.99H) of the post-critical galloping, are depicted in Figure 2. The effective wind attack angle α_{eff}, based on the quasi-steady theory and employed to plot the hysteresis loops, is defined in Figure 1, and can be calculated according to the following equation:

$$\alpha_{\text{eff}} = \alpha + \Delta\alpha \tag{1}$$

where $\Delta\alpha = -\arctan(\dot{h}/U)$ is the motion-induced wind attack angle, $\dot{h}$ is the vibration velocity of the bluff body. For the sake of comparison, the steady lift force curve for the static bluff body is also reported in Figure 2. At small vibration amplitude, the C_L-α_{eff} hysteresis loop is a plump ellipse around the steady force curve, implying a linear unsteady behaviour. Then, the shape of the hysteresis loop gets distorted while the vibration amplitude increases. A reason for that is the nonlinear trend of the steady lift curve in the corresponding large range of α_{eff}.

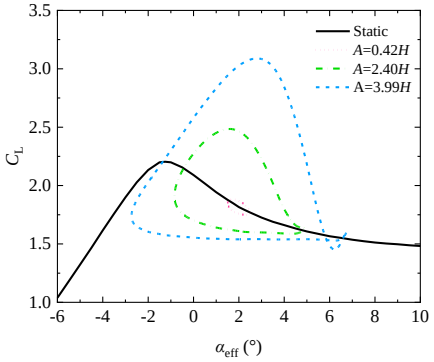

Figure 2. Hysteresis loops of the lift force for different vibration amplitudes at U/fH = 299.6.

Based on Fourier expansion, the galloping nonlinear aerodynamic force can be decomposed into multi-order harmonics as follows:

$$F_{\text{L}}(t) = \sum_{i=1}^{n} a_{\text{i}} \sin(i\omega t + \varphi_{\text{i}}) + \overline{F_{\text{L}}} \tag{1}$$

where $\overline{F_{\text{L}}}$ denotes the mean value of the lift force, i is the order of lift component, $\omega = 2\pi f$ is the circular frequency of vibration, a_{i} is the amplitude of the fluctuating force, and φ_{i} is its phase lag with respect to the body motion. Since higher-order force components do not do work on the simple harmonic motion of the structure, the force model can be simplified by ignoring the higher-order terms. Then it can be further written in the form:

$$F_{\mathrm{L,\,simp}}(t)=\rho U^2 H(KH_1^*\frac{\dot{h}}{U}+K^2H_4^*\frac{h}{H})+\overline{F_L} \tag{2}$$

where $K=\omega H/U$ is the reduced frequency; H_1^* and H_4^* denote the damping force coefficient and the stiffness force coefficient, respectively, and both of them are functions of reduced wind velocity as well as of vibration amplitude. H_1^* and H_4^* can be regarded as the nonlinear counterpart of the classical flutter derivatives for the galloping problem.

3. GALLOPING CALCULATION

3.1. Critical wind speed of galloping

Based on the unsteady nonlinear force model given in Equation (2), the vibration equation of the bluff body can be written as follows:

$$m(\ddot{h}+2\xi_0\omega_0\dot{h}+\omega_0^2h)=\rho U^2 H(KH_1^*\frac{\dot{h}}{U}+K^2H_4^*\frac{h}{H}) \tag{3}$$

where ξ_0 and ω_0 are the structural damping ratio and natural circular frequency of the bluff body, respectively. Then the critical wind speed can be calculated by satisfying $2m\xi_0\omega_0-\rho UHKH_1^*=0$.

The force coefficients H_1^* and H_4^* at different reduced wind velocity are obtained through CFD simulation of small-amplitude forced vibration (where A= 0.1H), as shown in Figure 3. And the critical wind speed of galloping is calculated and compared with that obtained through CFD simulation of free vibration, as well as the one calculated based on classical quasi-steady theory (as shown in Table 1). The calculation result of the unsteady force model agreed well with that of the CFD simulation, while the quasi-steady force model has a significant divergency (i.e., 30.1%) with the CFD simulation for this. In other word, the unsteady force model is applicable to calculate the critical wind speed of the unsteady galloping phenomenon, while the classical quasi-steady theory could lead to a significant calculation error.

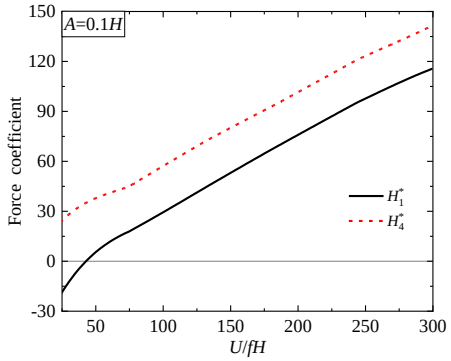

Figure 3. Variation of force coefficients with respect to reduced wind velocity.

Table 1. Comparison of critical wind speed between different methods

Method	CFD simulation	Unsteady force model	Quasi-steady force model
U_{cr}/fH	93.6	96.6	65.4
Error	-	3.2%	30.1%

3.2. Post-critical response of galloping

A serious of CFD simulations of forced vibration are carried out at various vibration amplitudes to obtain the amplitude-dependent H_1^* and H_4^* , as shown in Figure 4. Except for H_1^* at relatively small reduced wind speed, the variation trends of H_1^* and H_4^* with respect to the vibration amplitude are very similar between different reduced wind speeds. Specifically, H_1^* decreases monotonically from a positive value to a negative one with respect to the vibration amplitude, implying that the

aerodynamic damping is negative at a small amplitude and becomes positive at a relatively large amplitude.

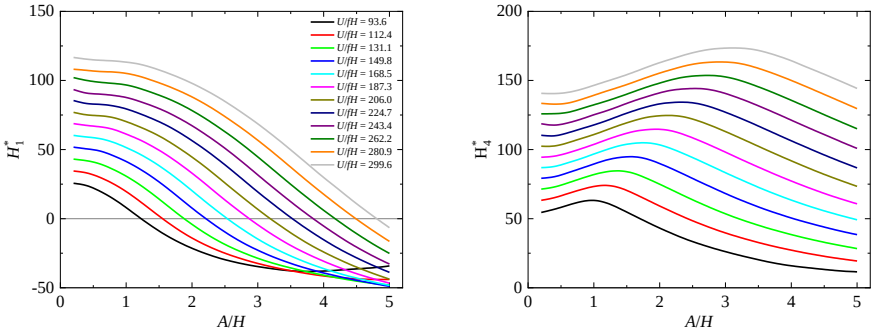

Figure 4. Variation of force coefficients with respect to vibration amplitude.

Based on the results of H_1^*, the aerodynamic damping can be calculated by $\xi_{\text{aero}} = 0.5\rho H^2 H_1^*/\text{m}$, as shown in Figure 5. Each contour line with positive value in Figure 5 denotes the amplitude-wind speed curve of post-critical galloping for a certain structural damping. In the sake of comparision, the amplitude results of free vibration at $\xi_0 = 0.15\%$ are also depicted in Figure 5 (i.e., the black dots). Generally, the calculation results agree well with the simulated one. Therefore, the post-critical response of the unsteady galloping can be effectively predicted based on the force model. Furthermore, for a bluff body with nonlinear structural damping (i.e., amplitude-dependent damping), the amplitude-wind speed curve can still be easily forecast through the contour map.

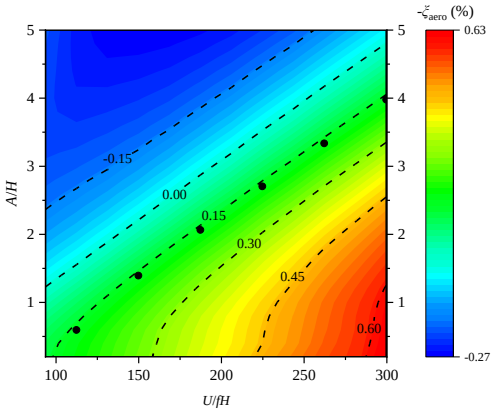

Figure 5. Aerodynamic damping contour with respect to vibration amplitude and reduced wind speed.

4. CONCLUSION

In post-critical galloping, nonlinearity of the self-excited lateral force is prominent only at large vibration amplitude, while unsteady characteristics are encountered at various vibration amplitudes even for a very high reduced wind velocity. The mathematical model based on amplitude-dependent flutter derivatives is introduced for the nonlinear galloping problem, and it is effective in calculations of both critical wind speed and post-critical response.

Acknowledgements

This study is sponsored by the National Science Foundation of China (No. 52025082) and China Scholarship Council (No. 202006130089), which are greatly acknowledged.

References

Wang C, Hua X, Huang Z, Tang Y, Chen Z (2021). Post-critical behavior of galloping for main cables of suspension bridges in construction phases. Journal of Fluids and Structures 101: 103205. https://doi.org/10.1016/j.jfluidstructs.2020.103205.

Tang Y (2015). Nonlinear self-excited forces of streamlined box deck and nonlinear flutter response. PhD thesis, Southwest Jiaotong University, Chengdu, China.